DTIC FILE COPY

(4)

ARL-STRUC-TM-503

AR-005-590

AD-A212 573

AUSTRALIA

DEPARTMENT OF DEFENCE

DEFENCE SCIENCE AND TECHNOLOGY ORGANISATION

AERONAUTICAL RESEARCH LABORATORY

MELBOURNE, VICTORIA

Aircraft Structures Technical Memorandum 503

EVALUATION OF A DAMAGED F/A-18 HORIZONTAL STABILATOR (U)

by

J. PAUL

Approved for Public Release

FEBRUARY 1989

89 9 18 059

AR-005-590

DEPARTMENT OF DEFENCE
DEFENCE SCIENCE AND TECHNOLOGY ORGANISATION
AERONAUTICAL RESEARCH LABORATORY

Aircraft Structures Technical Memorandum 503

EVALUATION OF A DAMAGED F/A-18 HORIZONTAL STABILATOR (U)

by

J. PAUL

SUMMARY

This paper describes the results of a static and dynamic structural test on a damaged F/A-18 Horizontal Stabilator. The structure was subjected to incremental static loading and the strains were recorded at each load increment. The structure was then vibrated at its fundamental bending frequency and the thermal emission profile of the critical area was measured using SPATE.

DSTO ARL MELBOURNE

POSTAL ADDRESS: Director, Aeronautical Research Laboratory,
P.O. Box 4331, Melbourne, Victoria, 3001, Australia

CONTENTS

1. INTRODUCTION

The repair of a damaged Royal Australian Air Force (RAAF) F/A-18 horizontal stabilator has been incorporated into the Composite Repair Engineering Development Program (CREDP). CREDP is a joint program between the Canadian Forces (CF), the RAAF and the United States Navy (USN) to evaluate the repair capability of damaged composite components on the F/A-18. As part of this program the Aeronautical Research Laboratory (ARL) was tasked to develop a repair for the damaged horizontal stabilator, which was initially classed as unserviceable and unrepairable due to two fragment strikes from a tracer rocket.

The purpose of this work is to establish the structural degradation caused by the fragment strike to the horizontal stabilator. Two independent tests were carried out on the stabilator. The first test was a strain survey requiring the application of static loads, achieved by using air bags and the second was a thermal emission survey involving the application of a constant amplitude dynamic load.

2. DAMAGE DESCRIPTION

The F/A-18 horizontal stabilator comprises graphite/epoxy skins with fibres oriented in the 0° and ±45° directions with a reference axis shown in Figure 1. The skin is supported on a full-depth honeycomb. The stabilator is fully symmetric top and bottom and can be interchanged on either side of the aircraft. In the region of the damage the skin is 29 plies thick (3.68mm), but tapers off to 5 plies (0.64mm) at the leading edge.

The horizontal stabilator had incurred two strikes by fragments, approaching from the rear, near the leading edge, see Figure 1. Both fragments caused extensive local damage to the composite skin and underlying honeycomb, but neither fragment penetrated to the other side of the stabilator. As seen in Figure 1, the two damaged areas are roughly the same size and both strikes have caused additional delamination in the skin, see Figures 2 and 3. The damage zone was C-scanned to determine the amount of additional delamination. However, interpretation of the C-scan results was made

difficult due to the variation in the ply layup in the damage zone. The two damaged zones have been designated 'A' and 'B' and the relevant C-scan results can be seen in Figures 4 and 5. These figures show a band of internal delamination surrounding both holes and the surface plies which have been peeled away.

3. TEST RIG

In order to carry out the structural tests on the horizontal stabilator a test rig capable of applying the loads was required. Fortunately ARL had previously developed a test rig for a dynamic test on the horizontal stabilator, see Figure 6. The stabilator was mounted in the rig by means of the spindle, which is used to connect the stabilator to the aircraft. All bending loads are transferred to the rig via the spindle. A lever arm connected to the root of the stabilator transfers all torque to the test rig.

The static loads applied to the structure were achieved by using two Firestone* air bags resting on the surface of the stabilator. An additional structure, consisting of steel I beams, was built around the test rig to allow the air bags to be mounted above and below the stabilator. Prior to this test, a pressure versus extension calibration test was performed on the air bags to determine the force that the air bags applied to the stabilator.

To investigate the stress concentration around the damage thermal emission scans were taken of the damaged region. This was performed using a SPATE 8000 (Stress Pattern Analysis by measurement of Thermal Emission) device which measures the thermal emission of a body undergoing a cyclic change in stress. Two electro-magnetic shakers were attached to the underside of the stabilator, at a position that allowed the fundamental bending mode, at approximately 14 Hz, to be excited. A mirror was used to reflect the resultant thermal emission to the SPATE detector unit. The mirror was isolated from the test rig and floor to avoid the problem of vibration.

This approach relies on the coupling of the thermal and mechanical energy. In general a region with a high energy density, often referred to as a hot spot, will give rise

* Registered trade mark.

to a region with a large thermal emission. In particular a hole, delamination damage or a crack in a uniformly stressed component can be immediately seen as it results in a large change in the thermal emission profile. If damage is not structurally significant, i.e. it does not result in a significant change in the local stress field, it will not result in a significant change in the thermal emission profile.

As a result the thermal emission profile is thought to be a particularly valuable tool in assessing the structural significance of damage, in contrast to other more 'passive' non-destructive techniques such as C-scan, X-ray etc, which only provide information on the geometry of the damage and not its structural significance. Indeed the thermal emission profile 'actively' reflects the interaction of the damage with the structure, material, local geometry and load in a non-dest. :ctive fashion. As such it is particularly well suited to the present investigation and will be used to evaluate the structural significance of the fragment damage and to locate other damage locations.

4. INSTRUMENTATION

Four strain gauge rosettes were located in a rectangular pattern around the damage zone and in the corresponding location on the undamaged skin. The gauges in each rosette were aligned in the direction of the 0° and ± 45° fibres; see Figure 1. Two displacement transducers were placed half way between the left hand inboard rosettes (1 and 2), in the 0° fibre direction, as seen in Figures 7 and 8. The gauge length of the displacement transducers was 385mm. The strain gauge rosettes and displacement transducers were positioned so as to evaluate the change in compliance of the structure due to the major damage.

Displacement and pressure transducers were required to measure the extension and pressure for each air bag. The force applied by each air bag is a function of these two variables and was read off the calibration graph shown in Figure 9. The root bending moment (RBM) was calculated and used as the reference load applied to the structure. Three extra displacement transducers were attached to the stabilator at the tip, leading and trailing edges, see Figure 7, to measure tip displacement and torque induced by the applied load. A HP9816 data acquisition system was used to record the resulting 33

channels of data.

5. TEST DESCRIPTION

The first stage of the investigation involved the application of a static load by incrementing the air bag pressure in steps of 10 kPa. The maximum load applied to the structure was not considered to be critical as the primary objective was a comparison between the strains and the compliance on the top and bottom surfaces of the stabilator. Initially, the air bags were placed underneath the stabilator, producing tension in the damaged surface skin, and a dummy loading and unloading run was performed to allow the structure to settle. Several loading and unloading runs were made in this configuration with strain gauge and transducer readings being conducted at each increment of pressure. The loading was then repeated with the air bags re-configured above the stabilator producing a compressive load in the damaged surface.

After completion of the these static runs, an aluminium patch, 310mm long x 100mm wide and 1mm thick, was bonded onto the undamaged surface with its longitudinal centre line directly underneath the displacement transducer. The structure was then loaded as described above. The purpose of applying a patch was to examine the effect of the neutral axis shift and the local secondary bending induced by an external patch. In the absence of local secondary bending and if the neutral axis shift is negligible then the strain reduction, due to the patch, should be proportional to the change in nett sectional stress.

The second stage of the investigation was the thermal emission survey of the damaged zone using SPATE. For this test, the air bags were removed and two large electromagnetic shakers were positioned on either side of the stabilator and an accelerometer was located at the tip to allow the tuning of the fundamental bending frequency. Several thermal emission scans were taken of the damage zone with the wing vibrating at its fundamental bending mode at 14 Hz.

6. RESULTS AND DISCUSSION

The Ultimate Bending Moment (UBM) and the Design Limit Bending Moment (DLBM) for the horizontal stabilator are 1065 kip-in (120.3 kNm) and 710 kip-in (80.2 kNm) respectively, see Reference 1. The RBM was calculated for each load increment and the test achieved 31% (47%) and 26% (39%) UBM (DLBM) in tension and compression respectively.

The strain survey results for one loading cycle are shown in Tables 1 and 2 for the unpatched runs and Tables 3 and 4 for the patched runs. All strain values are presented in microstrain. Tables 1 and 2 show that there is in most cases no structurally significant difference between the top and bottom surface strain gauge results in the 0° fibre direction. However, there is a 24% to 27% reduction in gauge D2 0° , which is located close to the edge of the damage 'A', depending upon the value of the RBM. This may be due to the gauge being shielded by the damage. The compliance readings, shown at the bottom of the tables as 'U strain' for the undamaged surface strain and 'D strain' for the damaged surface strain, result in no significant difference between top and bottom surfaces. This implies that the local compliance has not been affected by the damage and indicates that there is little structural degradation.

Tables 3 and 4 show the tension and compressive strain surveys for the structure after the patch had being applied. Based on the change in the nett sectional stress it was anticipated that the patch would reduce the strain in the upper surface of the stabilator, as measured by the displacement transducers, by 27%. Comparing the 'U strains' from Tables 2 and 4 we see a reduction of 24% to 30% in strain, see Table 5, and the difference is within experimental error. This implies that there is no detectable local secondary bending and that the neutral axis shift, due to the external patch, was insignificant.

With the upper surface patched, the damaged surface strains, in the 0° fibre direction vary less than 7%. However, the two rosettes U2 and U4 closest to the leading edge showed a 17% and 13% reduction respectively, see Table 5. All recorded strains were essentially linear with load and the increase in strain due to the damage was less than 5%.

To investigate the stress concentration around the damage further, a number of detailed thermal emission scans were taken. The SPATE photo is orientated as a mirror image of Figure 8. The results of one of these scans is shown in Figures 11, and to assist the reader in interpreting the picture, an overlay is provided Figure 10. Examination of this figure reveals that, as indicated by the strain gauge and compliance measurements, there was no 'classical' stress concentration affect around the damage. There is also a region, in the vicinity of gauge U2, which gave a spurious thermal emission reading. This spurious reading vanished when the structure was excited at 12 Hz.

7. CONCLUSIONS

The strain survey conducted indicates that there is minimal structural degradation resulting from the fragment strikes. The results also show that the damage produces no measurable change in local compliance. The thermal emission results confirm these measurements and do not show the classical stress concentration around the fragment holes. Since the damage does not appear to compromise the compliance of the structure a simple externally bonded repair should suffice. This investigation has revealed that such a repair will not result in a significant change in the local neutral axis or an associated increase in secondary bending.

REFERENCES

1. 'Spanish Production Stabilator Fatigue and Static Demonstrator Tests' McDonnell Aircraft Company, LMA03.04-031, pp17

2. Jones R., Broughton W., Mousley R.F. and Potter R.T., 'Compression Failures of Damaged Graphite Epoxy Laminates', Composite Structures Vol. 3, pp167–186, (1985).

3. Molent, L. and Paul, J., 'Applications of energy density theory in cyclic plasticity', ARL-A/STRUCT-TM-469, Aeronautical Research Laboratory, Melbourne, Australia, August (1987) and Theoretical and Applied Fracture Mechanics, Vol. 10, pp43–48, (1988).

Table 1: Results for Damaged Surface in Tension.

R.B.M. (kNm)		0	11	20	29	38	29	20	0
Torque (kNm)		0	7	14	20	26	20	14	0
Gauge D1	+45	-3	153	292	411	545	423	299	-2
Gauge D1	0	-5	320	604	852	1126	873	616	-4
Gauge D1	-45	-4	61	116	164	218	167	116	-5
Gauge D2	+45	-4	72	134	188	246	192	136	-3
Gauge D2	0	-3	149	285	405	540	415	290	-3
Gauge D2	-45	-3	18	42	64	93	66	42	-5
Gauge D3	+45	-4	213	403	567	748	581	410	-4
Gauge D3	0	-5	521	979	1374	1810	1403	989	-16
Gauge D3	-45	-4	119	226	317	418	324	229	-4
Gauge D4	+45	-3	150	285	402	530	412	292	-1
Gauge D4	0	-4	328	622	878	1163	899	634	-2
Gauge D4	-45	-4	31	62	89	122	90	60	-5
Gauge U1	+45	-4	-148	-276	-391	-519	-403	-284	-4
Gauge U1	0	-6	-331	-620	-875	-1161	-897	-631	-5
Gauge U1	-45	-5	-87	-157	-219	-288	-221	-156	-3
Gauge U2	+45	-3	-145	-274	-389	-519	-400	-280	-3
Gauge U2	0	-3	-203	-377	-529	-697	-542	-384	-2
Gauge U2	-45	-4	16	36	57	82	61	40	-1
Gauge U3	+45	-4	-214	-403	-572	-761	-588	-412	-4
Gauge U3	0	-5	-525	-988	-1396	-1855	-1430	-1004	-4
Gauge U3	-45	-2	-143	-271	-384	-511	-395	-277	-3
Gauge U4	+45	-3	-130	-241	-339	-448	-344	-242	-1
Gauge U4	0	-3	-330	-617	-868	-1147	-890	-629	-4
Gauge U4	-45	0	-3	-7	-9	-13	-10	-7	0
U Strain		-8	-463	-882	-1242	-1651	-1289	-913	-19
D Strain		-9	448	877	1234	1645	1268	888	3

Table 2: Results for Damaged Surface in Compression.

R.B.M. (kNm)		0	-9	-18	-25	-31	-25	-18	-9	0
Torque (kNm)		0	-6	-13	-18	-22	-18	-13	-6	0
Gauge D1	+45	-1	-131	-258	-361	-453	-369	-269	-144	-1
Gauge D1	0	-1	-263	-516	-717	-899	-732	-531	-283	-1
Gauge D1	-45	0	-49	-95	-132	-164	-132	-96	-51	-1
Gauge D2	+45	-1	-64	-125	-175	-219	-176	-127	-69	-1
Gauge D2	0	0	-119	-232	-321	-400	-327	-240	-129	-1
Gauge D2	-45	-1	-12	-24	-32	-39	-33	-30	-17	-1
Gauge D3	+45	0	-182	-356	-496	-622	-505	-366	-194	-1
Gauge D3	0	-1	-423	-827	-1151	-1437	-1156	-831	-434	-2
Gauge D3	-45	0	-95	-186	-259	-325	-262	-191	-101	-2
Gauge D4	+45	-1	-126	-246	-344	-431	-351	-256	-138	-1
Gauge D4	0	-1	-261	-508	-705	-878	-717	-522	-281	-1
Gauge D4	-45	-1	-25	-47	-63	-78	-64	-48	-27	-1
Gauge U1	+45	0	119	232	322	401	328	238	127	-1
Gauge U1	0	-1	260	507	705	877	714	518	275	-1
Gauge U1	-45	0	60	119	165	204	164	118	60	-1
Gauge U2	+45	-1	113	219	304	376	308	224	119	-1
Gauge U2	0	-1	161	316	440	550	446	320	168	-1
Gauge U2	-45	-1	-16	-27	-36	-42	-39	-37	-24	-1
Gauge U3	+45	-1	171	333	463	573	467	339	180	-1
Gauge U3	0	-1	405	790	1097	1357	1107	804	429	-1
Gauge U3	-45	-1	112	218	302	373	304	220	117	-1
Gauge U4	+45	-1	93	182	252	311	252	181	95	-1
Gauge U4	0	-1	257	502	702	872	708	513	272	0
Gauge U4	-45	0	-3	-6	-8	-10	-8	-6	-3	0
U Strain		1	370	734	1038	1285	1067	788	438	0
D Strain		0	-363	-719	-1016	-1260	-1041	-754	-403	0

Table 3: Results for Damaged Surface in Tension - Top surface patched.

R.B.M. (kNm)		0	11	20	29	21	0
Torque (kNm)		0	7	14	20	14	0
Gauge D1	+45	-2	157	294	425	301	-2
Gauge D1	0	-5	326	610	879	620	-6
Gauge D1	-45	-5	60	115	168	115	-7
Gauge D2	+45	-4	68	127	181	127	-4
Gauge D2	0	-1	156	293	426	299	-2
Gauge D2	-45	-1	24	50	78	52	-2
Gauge D3	+45	-4	222	414	596	421	-4
Gauge D3	0	-11	524	977	1404	989	-18
Gauge D3	-45	-5	114	215	310	219	-6
Gauge D4	+45	-4	157	296	426	301	-3
Gauge D4	0	-5	334	629	910	640	-5
Gauge D4	-45	-5	21	43	66	43	-5
Gauge U1	+45	-5	-146	-269	-390	-276	-6
Gauge U1	0	-6	-332	-615	-888	-627	-7
Gauge U1	-45	-5	-87	-157	-223	-157	-5
Gauge U2	+45	-4	-150	-279	-406	-285	-4
Gauge U2	0	-1	-195	-359	-518	-367	-1
Gauge U2	-45	1	27	54	82	56	2
Gauge U3	+45	-5	-221	-410	-594	-417	-5
Gauge U3	0	-6	-527	-980	-1416	-996	-6
Gauge U3	-45	-4	-128	-239	-348	-246	-4
Gauge U4	+45	-4	-123	-227	-325	-230	-3
Gauge U4	0	-6	-306	-566	-815	-582	-8
Gauge U4	-45	0	-4	-6	-10	-7	0
U Strain		-6	-410	-760	-1086	-761	16
D Strain		4	468	878	1264	892	3

Table 4: Results for Damaged Surface in Compression – Top surface patched.

R.B.M. (kNm)		0	-12	-20	-29	-21	0
Torque (kNm)		0	-8	-14	-20	-14	0
Gauge D1	+45	-1	-163	-282	-394	-290	-5
Gauge D1	0	-2	-330	-568	-789	-579	-6
Gauge D1	-45	-1	-65	-110	-151	-111	-4
Gauge D2	+45	-2	-76	-130	-181	-131	-5
Gauge D2	0	-1	-152	-260	-360	-266	-3
Gauge D2	-45	-2	-24	-37	-49	-39	-4
Gauge D3	+45	-1	-227	-394	-549	-402	-5
Gauge D3	0	-2	-521	-902	-1251	-912	3
Gauge D3	-45	-1	-117	-201	-280	-205	-4
Gauge D4	+45	-1	-157	-275	-383	-281	-3
Gauge D4	0	-1	-325	-561	-777	-572	-4
Gauge D4	-45	-1	-27	-40	-55	-41	-3
Gauge U1	+45	-1	138	238	332	244	-3
Gauge U1	0	-2	315	540	751	550	-5
Gauge U1	-45	-1	75	128	178	128	-5
Gauge U2	+45	-1	138	237	328	242	-3
Gauge U2	0	-2	191	329	459	335	-4
Gauge U2	-45	-1	-24	-40	-52	-41	-4
Gauge U3	+45	-2	209	359	498	364	-4
Gauge U3	0	-2	494	851	1178	864	-5
Gauge U3	-45	0	118	205	283	210	0
Gauge U4	+45	-1	109	187	260	189	-4
Gauge U4	0	-1	289	501	698	513	1
Gauge U4	-45	0	-4	-6	-9	-6	0
U Strain		0	371	641	888	652	-8
D Strain		0	-439	-779	-1098	-816	-14

Table 5: Percentage difference between interpolated damaged surface strains and the patched damage surface strains for the 0° gauges, +ve percentage represents a strain reduction.

R.B.M. (kNm)	12	20	29	21	Mean
Torque (kNm)	8	14	20	14	Mean
D1	6	3	4	1	3
D2	4	1	2	-1	2
D3	9	4	5	3	5
D4	-10	-3	-4	-2	-5
U1	-11	-7	-6	-5	-7
U2	24	15	13	15	17
U3	10	6	5	4	6
U4	16	12	13	10	13
U strain	30	25	25	24	26

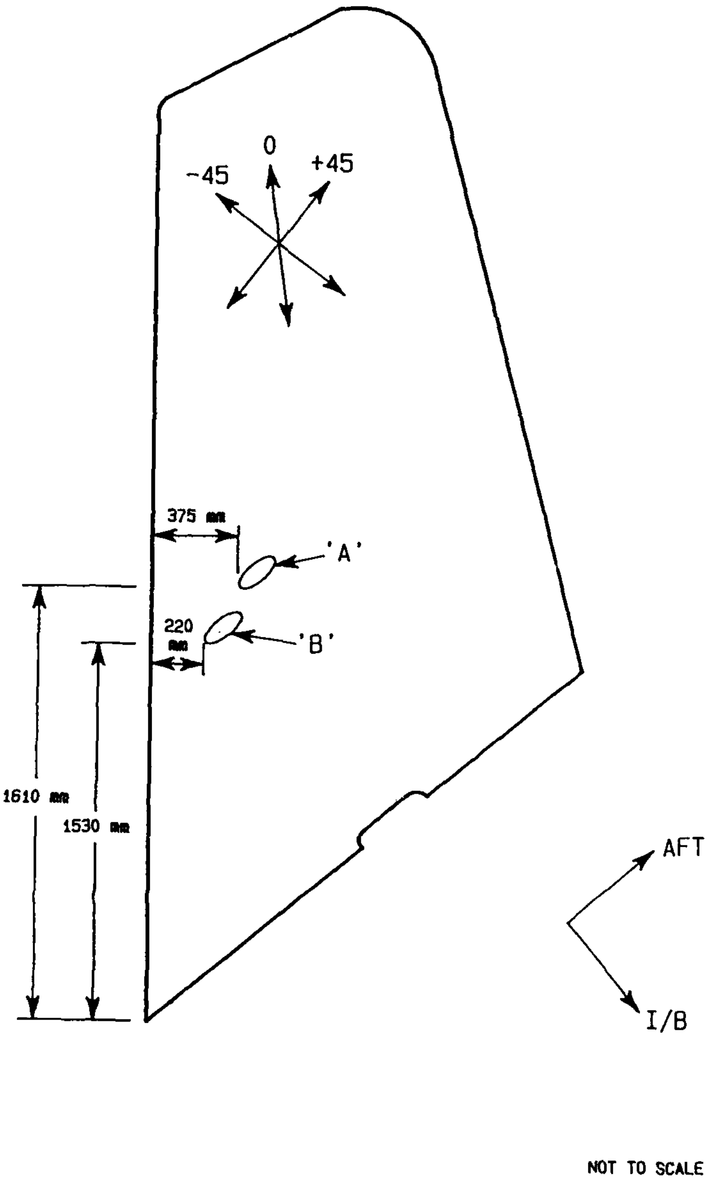

FIGURE 1 F/A-18 HORIZONTAL STABILATOR WITH DAMAGE LOCATION

Approximately full scale

FIGURE 2 CLOSE UP OF DAMAGE ZONE 'A'

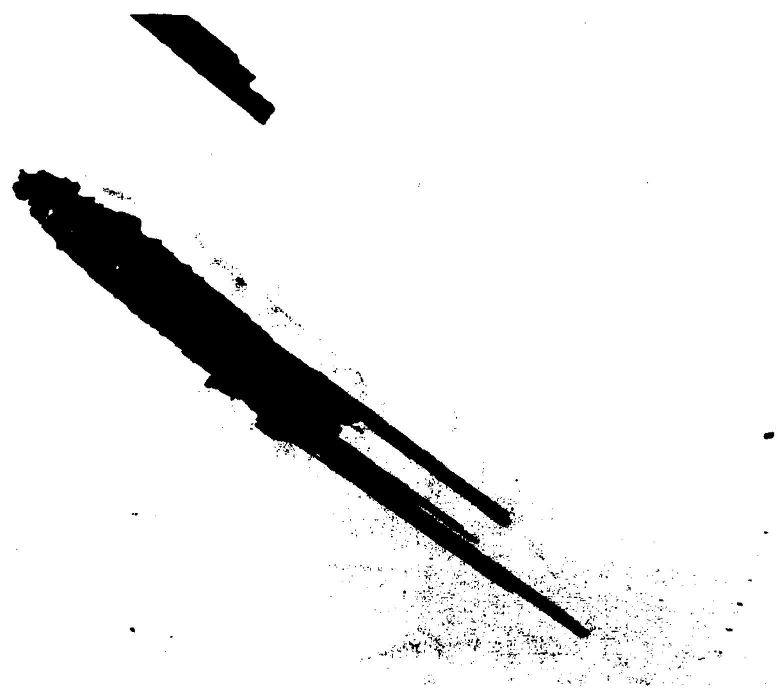

Approximately full scale

FIGURE 3 CLOSE UP OF DAMAGE ZONE 'B'

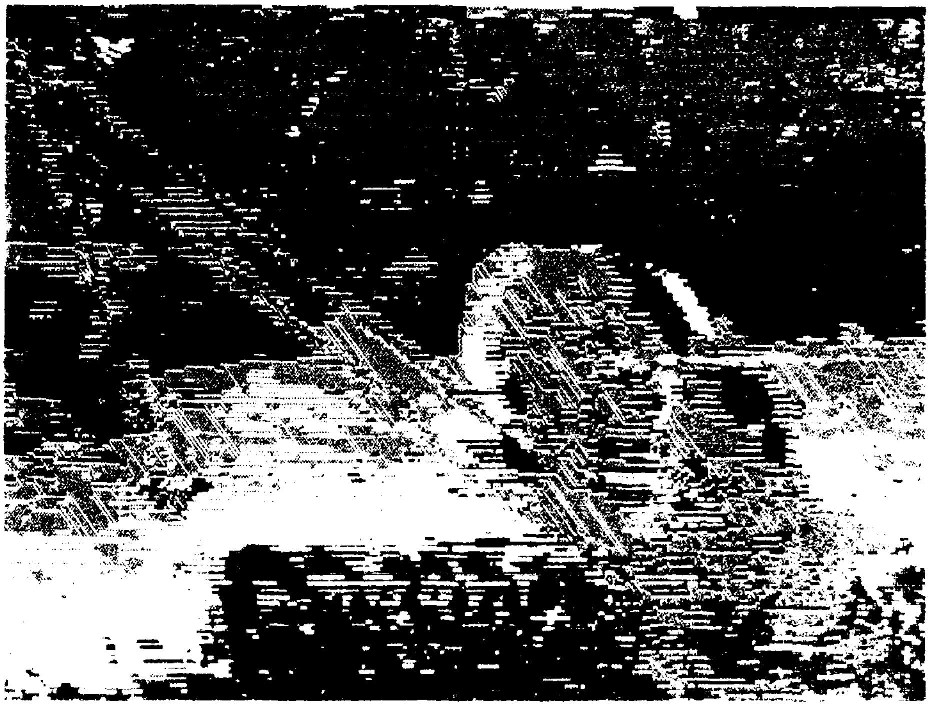

Scale 1:1

FIGURE 4 C-SCAN RESULT FOR DAMAGE ZONE'A'

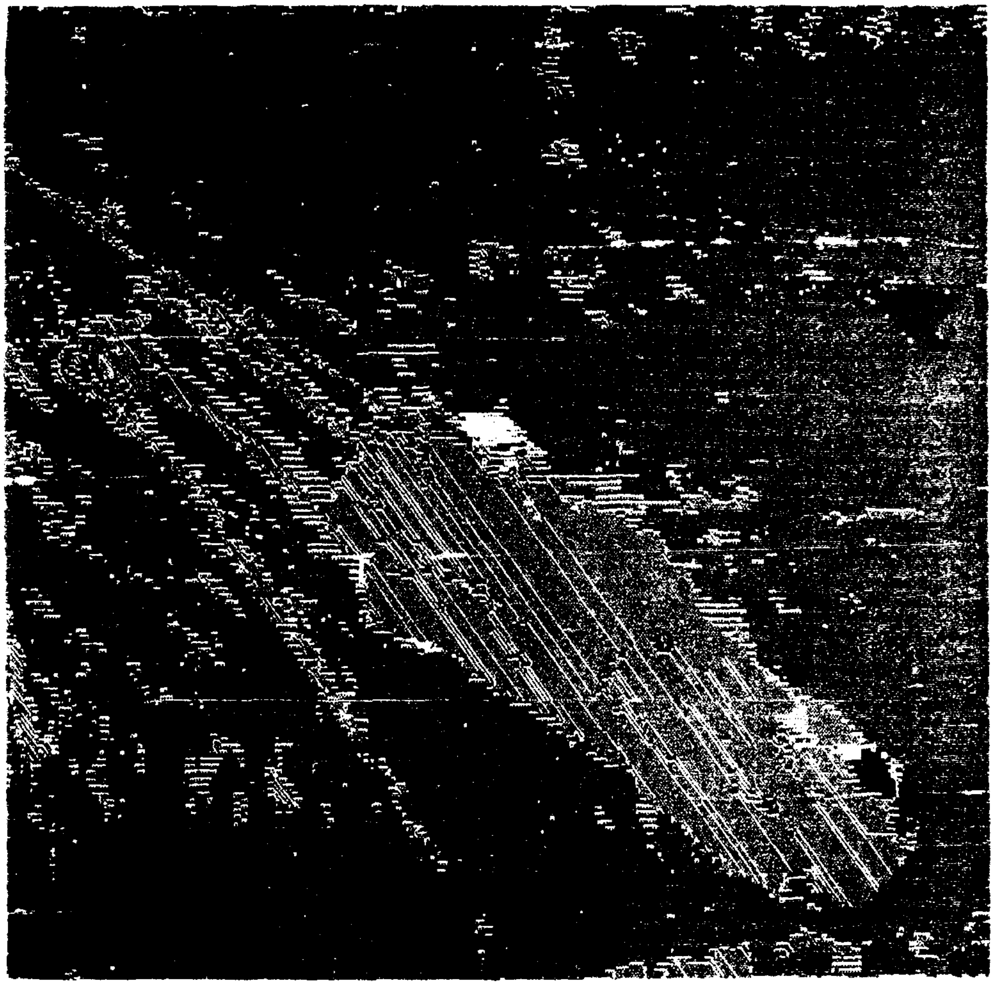

Scale 1:1

FIGURE 5 C-SCAN RESULT FOR DAMAGE ZONE 'B'

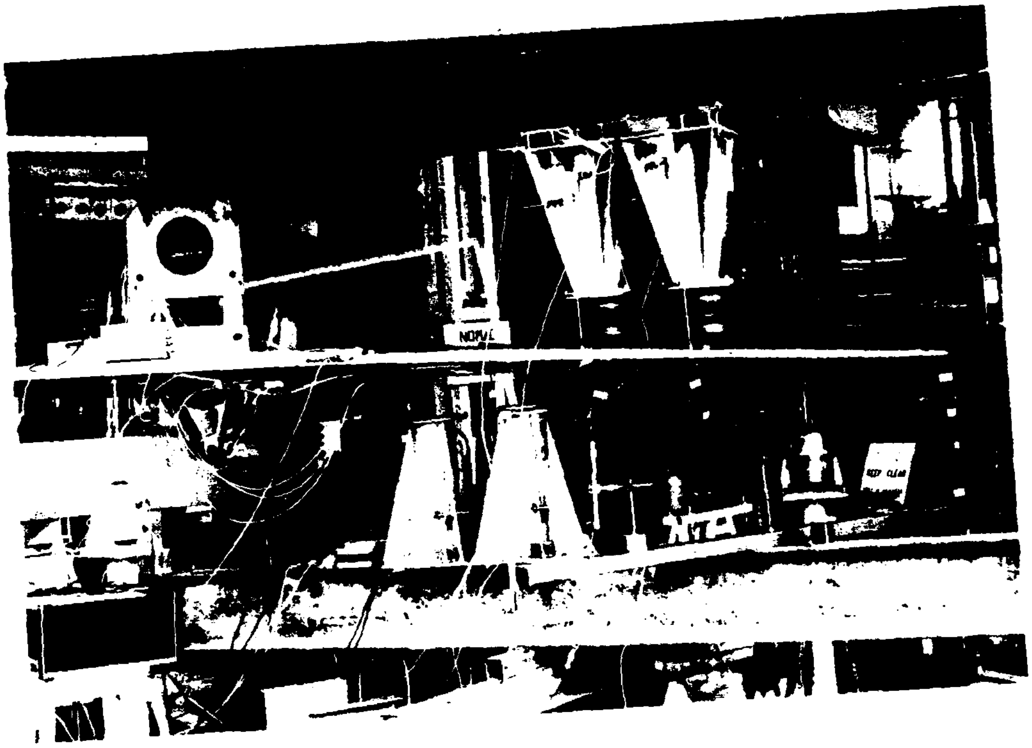

FIGURE 6 F/A-18 HORIZONTAL STABILATOR TEST RIG WITH AIR BAGS MOUNTED ABOVE

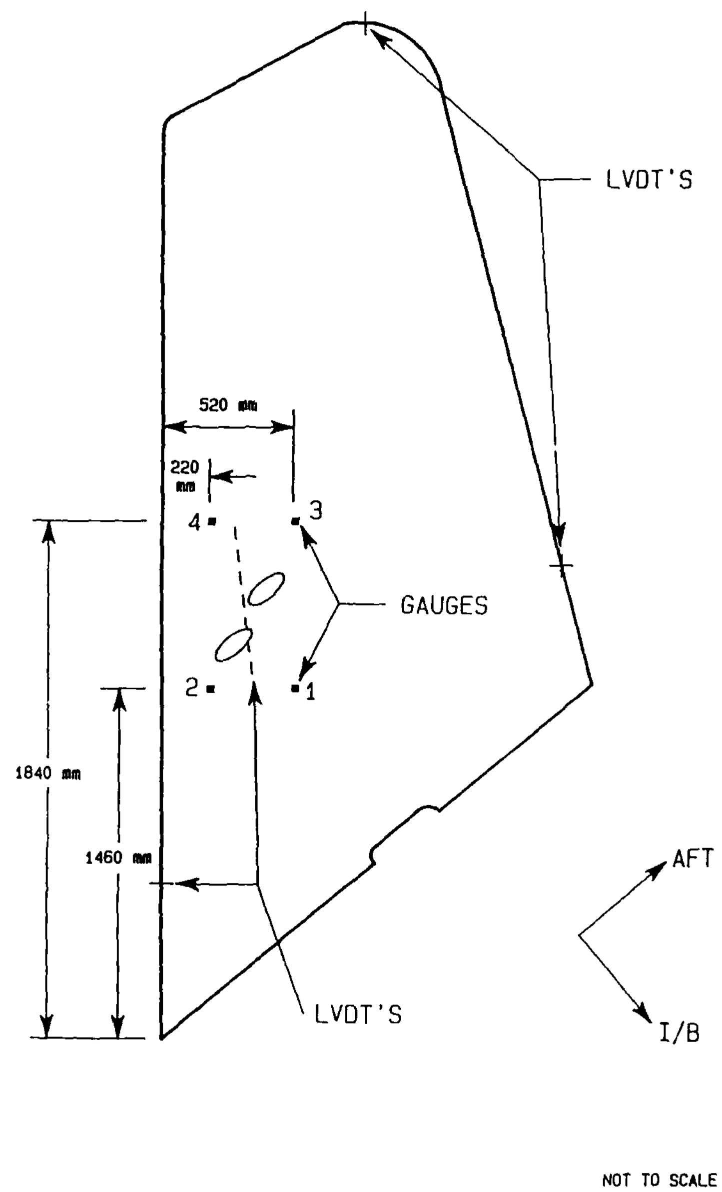

FIGURE 7 LOCATION OF STRAIN GAUGES AND DISPLACEMENT TRANSDUCERS

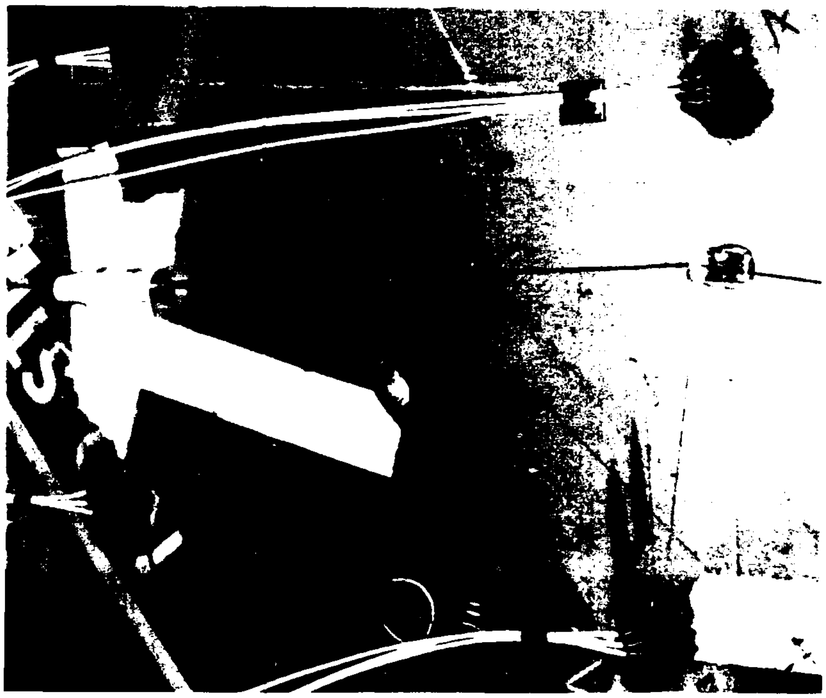

FIGURE 8 STRAIN GUAGE AND DISPLACEMENT TRANSDUCER POSITION AROUND THE DAMAGE

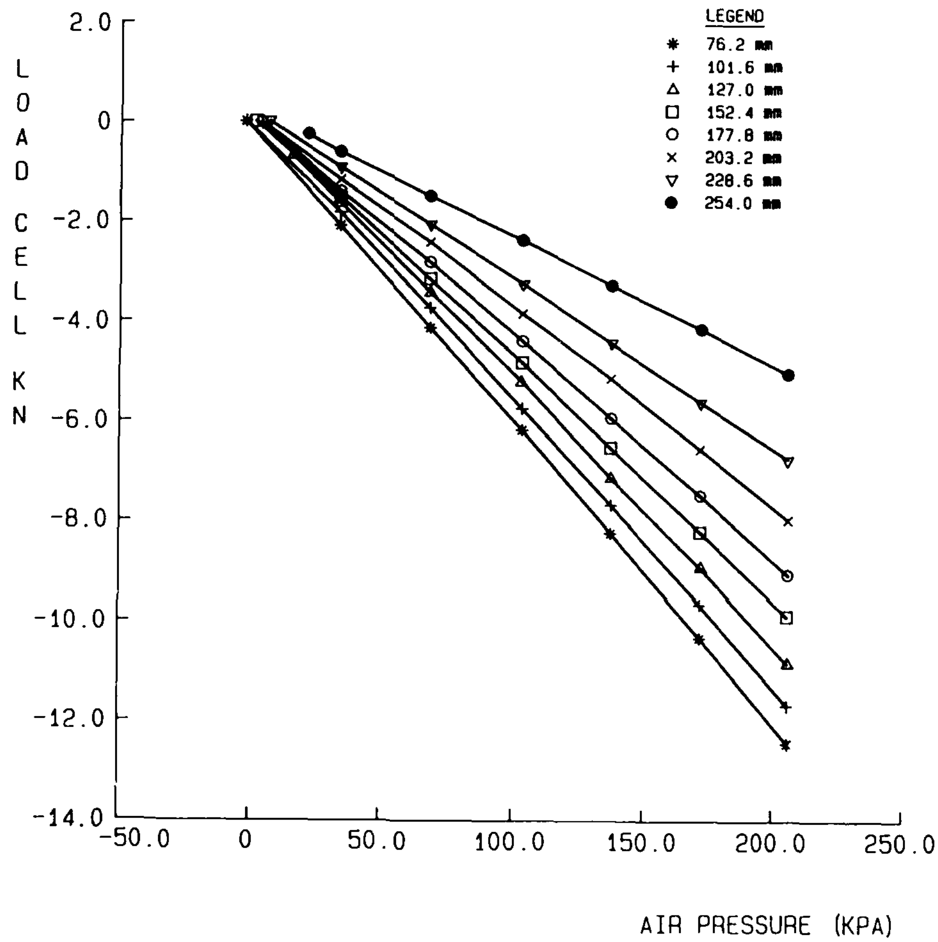

FIGURE 9 CALIBRATION CHART FOR THE FIRESTONE AIR BAG

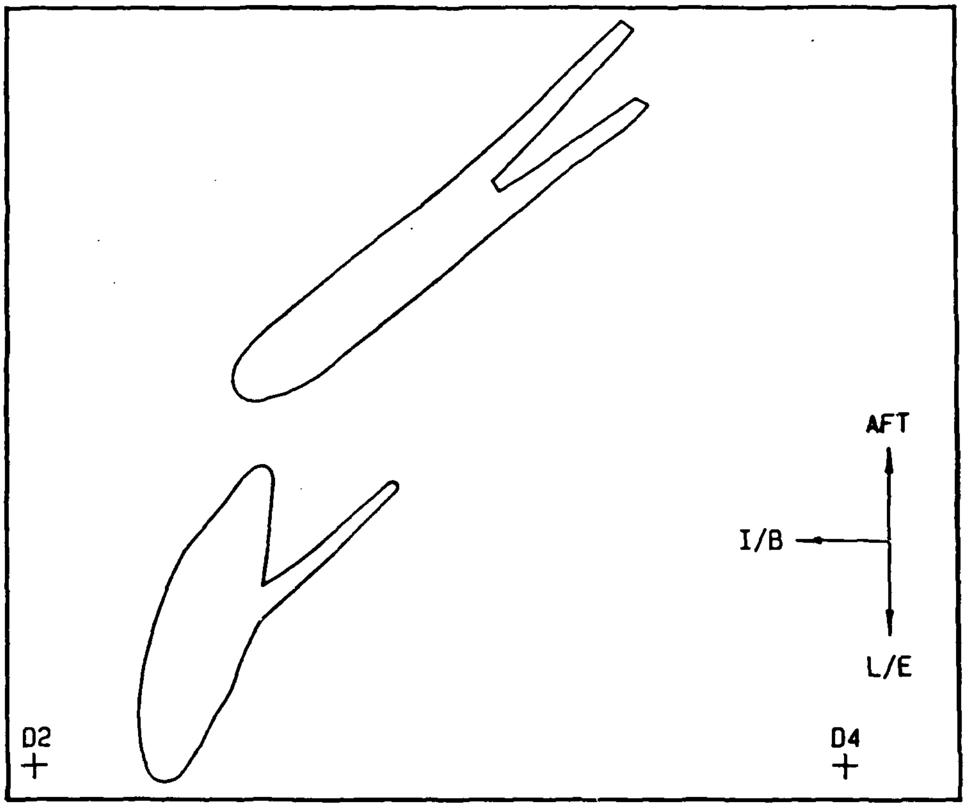

+ - Approximate qauge position.

Figure 10: Location of damage in Figure 11.
Mirror image of Figure 8.

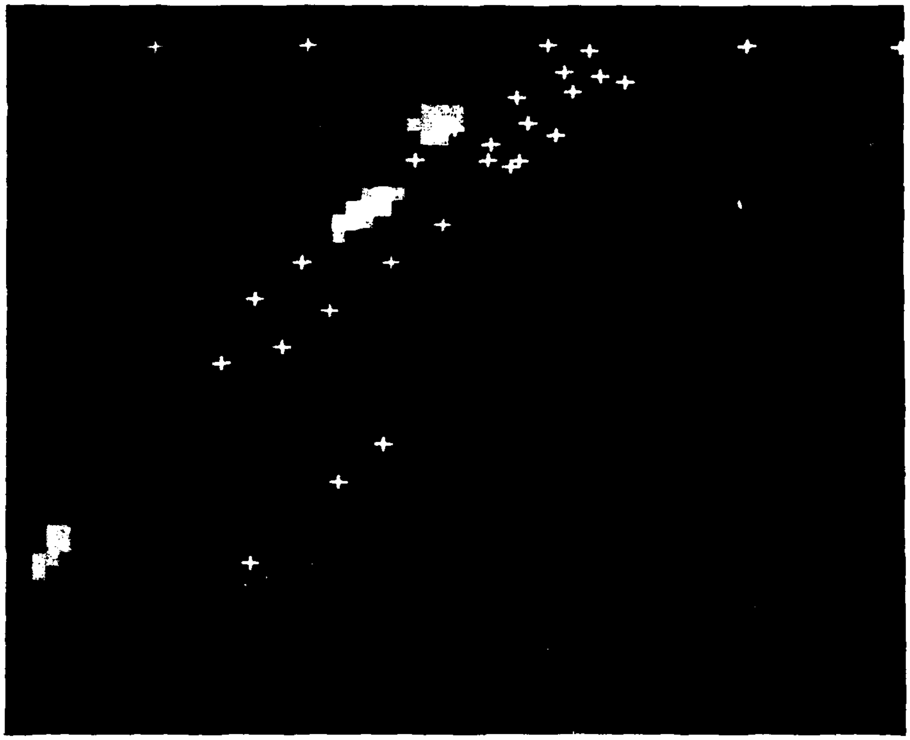

FIGURE 11 SPATE PICTURE OF DAMAGE ZONE

DISTRIBUTION

AUSTRALIA

Department of Defence

Defence Central
- Chief Defence Scientist
- FAS Science Corporate Management (shared copy)
- FAS Science Policy (shared copy)
- Director, Departmental Publications
- Counsellor, Defence Science, London (Doc Data Sheet Only)
- Counsellor, Defence Science, Washington (Doc Data Sheet Only)
- S.A. to Thailand MRD (Doc Data Sheet Only)
- S.A. to the DRC (Kuala Lumpur) (Doc Data Sheet Only)
- OIC TRS, Defence Central Library
- Document Exchange Centre, DISB (18 copies)
- Joint Intelligence Organisation
- FAS Defence Industry and Material Policy

Aeronautical Research Laboratory
- Director
- Library
- Chief - Aircraft Structures
- Divisional File - Aircraft Structures
- Author: J. Paul
- R. Jones
- A. Baker
- J. Roberts
- L. Molent
- N. Bridgford

Materials Research Laboratory
- Director/Library

Defence Science & Technology Organisation - Salisbury
- Library

WSRL
- Maritime Systems Division (Sydney)

Navy Office
- Navy Scientific Adviser (3 copies Doc Data sheet only)
- Aircraft Maintenance and Flight Trials Unit
- RAN Tactical School, Library
- Director of Naval Aircraft Engineering
- Director of Naval Air Warfare
- Superintendent, Aircraft Maintenance and Repair
- Director of Naval Ship Design

Army Office
- Scientific Adviser - Army (Doc Data sheet only)
- Engineering Development Establishment, Library
- US Army Research, Development and Standardisation Group

Air Force Office
Air Force Scientific Adviser
Aircraft Research and Development Unit
Scientific Flight Group
Library
Engineering Division Library
Director General Aircraft Engineering - Air Force
Director General Operational Requirements - Air Force
AIRENG5A
SQNLDR A.S. Morrison
HQ Air Command (SMAINTSO)
HQ Support Command (SLENGO)

Department of Transport & Communication
Library

Statutory and State Authorities and Industry
Civil Aviation Authority

CANADA

National Research Council of Canada
S. Hall

UNITED STATES OF AMERICA

Naval Aviation Depot
J. Longrig

SPARES (10 copies)
TOTAL (66 copies)

AL 149 DEPARTMENT OF DEFENCE

DOCUMENT CONTROL DATA

PAGE CLASSIFICATION
UNCLASSIFIED

PRIVACY MARKING

1a. AR NUMBER	1b. ESTABLISHMENT NUMBER	2. DOCUMENT DATE	3. TASK NUMBER
AR-005-590	ARL-STRUC-TM-503	FEBRUARY 1989	AIR 87/035

4. TITLE
EVALUATION OF A DAMAGED F/A-18 HORIZONTAL STABILATOR

5. SECURITY CLASSIFICATION (PLACE APPROPRIATE CLASSIFICATION IN BOX(S) IE. SECRET (S), CONF.(C) RESTRICTED (R), UNCLASSIFIED (U)).

DOCUMENT	TITLE	ABSTRACT
U	U	U

6. NO. PAGES
26

7. NO. REFS.
3

8. AUTHOR(S)
J. PAUL

9. DOWNGRADING/DELIMITING INSTRUCTIONS
Not applicable

10. CORPORATE AUTHOR AND ADDRESS
AERONAUTICAL RESEARCH LABORATORY
P.O. BOX 4331, MELBOURNE VIC 3001

11. OFFICE/POSITION RESPONSIBLE FOR:

SPONSOR RAAF
SECURITY -
DOWNGRADING -
APPROVAL CSTD

12. SECONDARY DISTRIBUTION (OF THIS DOCUMENT) Approved for public release.

OVERSEAS ENQUIRIES OUTSIDE STATED LIMITATIONS SHOULD BE REFERRED THROUGH ASDIS, DEFENCE INFORMATION SERVICES BRANCH, DEPARTMENT OF DEFENCE, CAMPBELL PARK, CANBERRA, ACT 2601

13a. THIS DOCUMENT MAY BE ANNOUNCED IN CATALOGUES AND AWARENESS SERVICES AVAILABLE TO....
No limitations

13b. CITATION FOR OTHER PURPOSES (IE. CASUAL ANNOUNCEMENT) MAY BE [X] UNRESTRICTED OR [ ] AS FOR 13a.

14. DESCRIPTORS

Stabilators,
F/A-18 aircraft,
Statis tests,
Dynamic tests,
Static loads,
Thermal emission.
Australia

15. DRDA SUBJECT CATEGORIES
0051C

16. ABSTRACT

This paper describes the results of a static and dynamic structural test on a damaged F/A-18 Horizontal Stabilator. The structure was subjected to incremental static loading and the strains were recorded at each load increment. The structure was then vibrated at its fundamental bending frequency and the thermal emission profile of the critical area was measured using SPATE. Keywords.

PAGE CLASSIFICATION UNCLASSIFIED
PRIVACY MARKING

THIS PAGE IS TO BE USED TO RECORD INFORMATION WHICH IS REQUIRED BY THE ESTABLISHMENT FOR ITS OWN USE BUT WHICH WILL NOT BE ADDED TO THE DISTIS DATA UNLESS SPECIFICALLY REQUESTED.

16. ABSTRACT (CONT.)		
17. IMPRINT AERONAUTICAL RESEARCH LABORATORY, MELBOURNE		
18. DOCUMENT SERIES AND NUMBER AIRCRAFT STRUCTURES TECHNICAL MEMORANDUM 503	19. COST CODE 361125	20. TYPE OF REPORT AND PERIOD COVERED
21. COMPUTER PROGRAMS USED		
22. ESTABLISHMENT FILE REF.(S)		
23. ADDITIONAL INFORMATION (AS REQUIRED)		